Molecular BioSystems

Accepted Manuscript

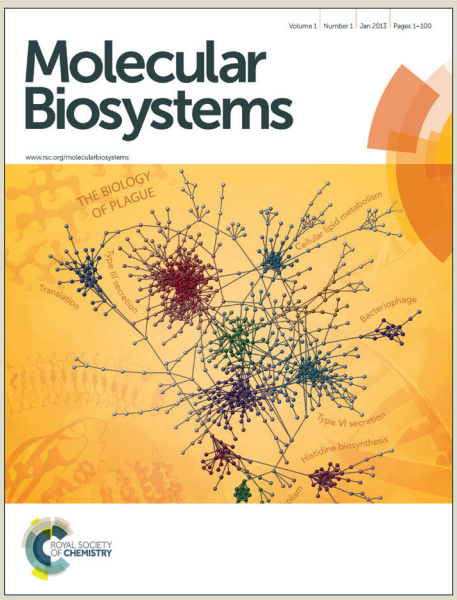

ROYAL SOCIETY OF CHEMISTRY

www.rsc.org/molecularbiosystems

Binding Studies of L-3,4-Dihydroxyphenylalanine with Human Serum Albumin

Daniel Pushparaju Yeggoni, Rajagopal Subramanyam*

Department of Plant Sciences, School of Life Sciences, University of Hyderabad, Hyderabad 500046, India

*Corresponding author
Rajagopal Subramanyam
Department of Plant Sciences
School of Life Sciences
University of Hyderabad 500 046 India
Tel: +91-40-23134572
Fax: +91-40-23010120
Email:srgsl@uohyd.ernet.in

Abstract

L-Dopa had been used to increase dopamine concentrations in the treatment of Parkinson's disease and dopamine-responsive dystonia. The binding interaction between L-dopa (phytochemical) and human serum albumin (HSA) in simulated physiological conditions was investigated by spectroscopic and molecular modeling methods. The results revealed that L-dopa caused the fluorescence emission quenching of HSA through a static quenching procedure and binding constant obtained was $2.3\pm 0.01 \times 10^{4}$ M^{-1} which is corresponding to -5.9 kcal M^{-1} of free energy at 25 °C. Interestingly, L-dopa is not binding to the α-1-acidglycoprotein which is also a plasma protein, an acute phase protein. Further, circular dichroism results confirm that in the presence of L-dopa the secondary structure of HSA is altered due to partial unfolding of the protein. Importantly, the displacement experiment with site specific probes phenylbutazone (Site I) and ibuprofen (Site II) depicts that L-dopa binds particularly to site II on HSA. In addition, the molecular modeling results also confirmed that L-dopa is binding to subdomain IIIA of HSA and stabilized by hydrogen bonds and hydrophilic forces. Additionally, the molecular dynamics simulation studies showed that the HSA-L-dopa complex reaches an equilibration state at around 2 ns which indicates that the HSA-L-dopa complexes are much stable. Apparently, these results provided valuable information for pharmacological mechanisms of L-dopa *in vivo* conditions and play a pivotal role in development of L-dopa-inspired drugs.

Keywords: L-dopa; drug binding; fluorescence quenching; α-1-acid glycoprotein; human serum albumin; circular dichroism; molecular displacement; molecular docking; molecular dynamics

Introduction

Human serum albumin (HSA) is most important and abundant extracellular protein present in the human blood plasma and it constitutes about 60% of the total plasma proteins. It is produced in the liver. Since HSA comprises multiple binding sites in turn have exceptional ability to bind with number of exogenous and endogenous compounds that helps in transporting the compounds in the blood system to the target site. [1, 2] HSA is a globular protein, consists of 585 amino acids residues, total molecular mass of 67 KDa and a serum half-life of 20 days. It is having a single polypeptide chain which is stabilized by 17 disulphide bridges. Moreover, HSA structure consists of three structurally similar domains (I-III) and each domain further divided into subdomain A and B. There are two major designated drug binding sites on HSA i:e IIA and IIIA known as sudlow's site I and II, respectively, where in most of the heterocyclic and aromatic compounds bind with in these sites .[3-6] Due to the globular domain structural organization of HSA provides a variety of binding sites for various ligands making it an important determinant of pharmacokinetic behavior of several drugs. In general, HSA interacts reversibly with a wide range of therapeutic agents. Drugs with excessively high affinity for HSA are distributed slowly to sites of action and may not be efficiently eliminated. Interesting fact about HSA has a high affinity to various metals such as Cu^{2+} and Zn^{2+}, fatty acids, amino acids, metabolites (e.g.bilirubin) and many other drugs.[7-9] Recently discovered report revealed that even subdomain IB also actively participated in drug binding and thus, this domain is one of the potential drug binding sites[10]. We also reported that trans-feruloyl maslinic acid and 7-hydroxy-4-methyl

coumarin derivatives strongly bind to IB domain. [11, 12] The drug that are explicitly binds to subdomain IB is lidocaine, subdomain IIA i:e site I are warfarin, phenylbutazone and Iodipamide whereas drugs that bind specifically to subdomain IIIA i:e site II are ibuprofen, diazepam and pirprofen .[10, 13-15] Innumerable drugs would bound to these major binding sites with binding affinity range of 10^4–10^6 L mol^{-1}. [6]

L-Dopa ($C_9H_{11}NO_4$,) is a naturally occurring form of dihydroxyphenylalanine in some animals and humans. L-Dopa is found in: *Mucuna pruriens*, *Tamarindus indica*, *Sesbania bispinosa*, *Acacia leucophloea*, *Canavalia gladiate.* [16] L-dopa is a precursor to the neurotransmitters of dopamine, norepinephrine (noradrenaline), and epinephrine (adrenaline) collectively known as catecholamines. Apparently, it crosses the protective blood–brain barrier, whereas dopamine could not do this function. Consequently, treatment of Parkinson's disease the L-dopa is used to increase dopamine concentration [17] and dopamine-responsive dystonia. Once L-dopa has entered the central nervous system, it is converted into dopamine by the enzyme aromatic L-amino acid decarboxylase, also known as dopa decarboxylase. Pyridoxal phosphate (vitamin B_6) is required cofactor in this reaction, and may occasionally be administered along with L-dopa in the form of pyridoxine. Besides the central nervous system, L-dopa is also converted into dopamine within the peripheral nervous system. The resulting hyperdopaminergia causes many of the adverse side effects seen with sole L-dopa administration. To bypass these effects, it is standard clinical practice to co-administer (with L-dopa) a peripheral dopa decarboxylase inhibitor such as carbidopa or with a benserazide to prevent the peripheral synthesis of dopamine from L-dopa. L-dopa can be directly metabolized by catechol-O-methyl transrerase to 3-O-methyldopa, and then further to vanillactic acid. This metabolic pathway is non-existent in healthy body, but becomes important after peripheral L-dopa administration in

patients with Parkinson's disease or in the rare cases of patients with aromatic L-amino acid decarboxylase enzyme deficiency. L-phenylalanine, L-tyrosine, and L-dopa, are all precursors to the biological pigment melanin.

Apart from Parkinson's disease, L-dopa shown to be having anti-oxidant properties.[18] A dose of 1000 mg/kg bodyweight, L-dopa in rats (human dose equivalent 160mg/kg) is associated with an increased circulating testosterone after 7-14 days.[19] Further, it also shown to interact with other hormones like growth and luteinizing hormone.[20] Moreover, L-dopa exerted significant effects on glucose metabolism (causing marked hyperglycemia) and on arterial blood pressure. Interestingly, this compound used for improving attention deficit hyperactivity disorder (ADHD) by improving sleep disorder.

However, most of the drugs consumed by humans are bound to HSA which significantly influence the distribution, absorption and efficacy. Since L-Dopa is having enormous pharmacological importance, and it's binding to human serum proteins have not been well studied since it is an important drug carrier protein in the blood system. Therefore, the interaction of L-dopa, a phytochemical, with HSA is significantly important, as it can provide good information about the drug-protein complex stability and secondary structural changes which indeed would be of great pharmacological importance. Thus, for our study we have used a phytochemical, L-Dopa in order to understand the binding mechanism with HSA. To reach this we have used both biophysical and computational approach and emphasized the mode of binding of L-Dopa with HSA.

MATERIALS AND METHODS

Pure fat-free HSA (all are from Sigma Aldrich) stock solution was prepared by dissolving at a concentration of 1.5mM in a physiological aqueous solution 0.1 M phosphate buffer of pH 7.2 The stock prepared were according to the previous reports. [11, 21]Purified L-dopa (Fig. 1 insert) from *Mucuna pruriens* was purchased from Natural remedies Pvt., Ltd, Bangalore, India, with purity of 95%. Through our previous reports a solution containing 20% ethanol has no effect on the secondary structure of protein. As HSA has maximum absorption at pH 7.2 so the optimum physiological is set at that point for HSA.[11, 21] As result the optimal physiological conditions is maintained for all the experiments. All the chemical are purchased without further purification and are of high purity grade. The binding time of L-dopa with HSA was optimized by using fluorescence emission spectroscopy and found to be the incubation time was 5min and we have maintained the same incubation time for all further experiments. There is no protein precipitation upon titration of L-dopa with HSA which indicates that L-dopa and HSA mixture is transparent.

Fluorescence spectroscopy measurements

The steady state fluorescence emission spectra were collected on a Perkin Elmer LS-55 Fluorescence spectrometer (PerkinElmer corporate, USA) with 1 cm path length cuvette. Here, the HSA is excited at 285nm in order to minimize the impact of emission of Tyr, spectra were recorded and maintained at 25 ^{o}C temperature with a wavelength range of 300–500 nm. The band width of 5.0 nm is set for both excitation and emission light. A fixed concentration of HSA was 1nM, and various concentrations of L-dopa were 1 to 9 μM in 0.1M phosphate buffer with

pH 7.2 (physiological pH). Three independent experiments were conducted and identical spectra were obtained at each time.

Molecular displacement experiment

In displacement experiments, a solution of L-dopa was increasingly titrated with system of HSA and site markers (phenyl butazone and ibuprofen) where the concentration of HSA and site specific marker was 1:1. The concentrations of HSA and site specific markers were maintained at 1μM, the L-dopa concentrations were 0-9μM. The excitation and emission used for system (HSA-site specific marker) were 285nm and 360nm, respectively. The fluorescence emission quenching data were analyzed using modified Stern-Volmer equation .[22, 23]

Circular dichroism spectroscopy

Circular dichroism (CD) spectra were recorded with a JASCO J-815 spectropolorimeter and a quartz cell with a path length 0.02cm. Here the Far-UV spectra were measured over the wave length range of 195-260nm and were performed at temperature of 25 ^{o}C. Four scans were accumulated at a scan speed of 50 nm min^{-1}. The concentration of HSA was 0.001mM and concentration of L-dopa was 0.001, 0.005 and 0.009 mM. To analysis the secondary structural changes in the protein CDNN 2.2 software is used.

Molecular modeling and Docking

Molecular docking is an important technique to understand the binding mode of ligand. Docking studies were performed by using Autodock 4.2.3. The aim is to predict the predominant binding site for ligand with a protein of known three dimensional structure. Here the crystal structure co-ordinates for HSA (PDB ID : 1AO6) is downloaded from the RCSB Protein Data Bank. Chain A was selected, water molecules and ions were removed and all hydrogen atoms were added, to

functional groups with the appropriate geometry with in the protein in order to get proper protonation state of active site of the protein (which is reasonable at physiological pH of protein). The structure of HSA was protonated in InsightII (www.accelrys.com). Kollman united atom partial charges were assigned to HSA and then nonpolar hydrogen's of HSA were merged using AutoDock Tools. A 3D structure of L-dopa was built using Discovery Studio 3.5 software and whole geometry was optimized through Discovery Studio 3.5 software. Auto Dock uses a genetic algorithm (GA) and Lamarckian Genetic Algorithm (LGA) for internal conformational searches, and to generate conformations. [24-26] The parameters were at their default settings in the docking tab, the HSA and ligand are selected and GA parameters are set as the number of GA runs :30, population size:150 and number of generations for picking worst individual:10. To generate possible conformation LGA was implemented in Autodock to perform docking simulations. Among 30 conformations that are generated the lowest binding energy which is matching to the experimental values is taken for further simulation studies. [12, 27-29]

Molecular dynamics simulation

Molecular docking studies determine the mode of binding of ligand to the protein.

Molecular dynamics simulation **(**MD) simulation is important tools for understanding the function of biological molecules and physical basis of structure. It even provide an ultimate detail concerning individual particle motions as a function of time which in turn used to address specific queries about the properties of a model system. A 10000ps MD simulation was performed using GROMACS 4.0 package using the GROMOS96 43a l force field is used. [30, 31] The complex is immersed in the cubic box and SPC water was assigned for the water molecule. [30] The topology parameter of HSA was created by using the GROMAC'S program and topology

parameter of L-dopa were built by Prodrg. The entire solvated system was neutralized by adding sodium ions in the simulation and entire system was composed of 5843 atoms of HSA. L-dopa, $15Na^+$ counter ions and 69491 solvent atoms. In order to release the conflicting contacts, energy minimization was performed using steepest descent method of 1000 steps which is followed by conjugate gradient method for 1000 steps. MD simulations studies consists of two phase equilibration and production phase. In the first phase of equilibration the solute ptn, counter ions and L-dopa was fixed and the position restrained dynamics simulation of the system in which atom position of HSA were restrained at 300k for 30ps. Finally the full system is subjected to 10000ps, MD at 300k temperature and 1 bar pressure. Leaf frog algorithm with a time step of 2fs and atomic co-ordinates were recorded at every 0.5ps during the process of simulation. The MD simulation and analysis were performed OSCAR Linux cluster with 24 nodes (dual xeon processor) at BIF facility , University of Hyderabad.

Results and Discussion

Binding analysis of L-Dopa with HSA using fluorescence emission data

When a fixed concentration of HSA was titrated with various amounts of L-dopa, there is decrease in the fluorescence emission of HSA (Fig.1A). Here decrease in intensity is considered as quenching and quenching occurred in concentration dependent manner. The main emission of HSA is due to presence of single tryptophan (Trp) residue in subdomain IIA, however, there are other amino acids like tyrosine (Try) and phenylalanine residue but they have low quantum yield and thus, the major intrinsic fluorescence is due to presence of Trp which is located at 214 position of subdomain IIA. [32-34] Thus, fluorescence quenching upon addition of L-dopa causes quenching of fluorescence emission may be due to formation of HSA-L-dopa complexes.

However, upon addition of L-dopa, there is no peak shift of the maximum fluorescence at 360 nm indicating that no major structural alternations of HSA while binding with L-dopa. Aiding this information, there are numerous reports showed upon interaction of various ligand molecules with HSA showed quenching of the intrinsic fluorescence of HSA.[12, 29, 35-37] The results indicate that L-dopa binds to HSA which is a major drug carrier protein in the human blood plasma.

The HSA-L-dopa complex has increased absorbance at an excitation and emission wavelength of the measured fluorescence. In order to eliminate the inner filter effects and obtain accurate data absorbance, the measurements were done at excitation and emission fluorescence wavelengths. The fluorescence intensity was corrected by using the following equation.

$$\mathrm{Fcor} = \mathrm{Fobs10}\,(A_{exc} + A_{emi})/2 \quad \text{-[1]}$$

Where, F_{obs} and F_{cor} are the fluorescence intensity corrected and observed, A_{ex} and A_{em} represent the absorbance at the fluorescence excitation (285 nm) and emission wavelengths (360 nm) for HSA, respectively.

Further to elucidate the quenching mechanism which is denoted as static or dynamic quenching in the L-dopa-HSA complex F_o/F plotted against Q, the results are shown in the Fig.1B. The obtained plot between F_o/F and Q has a good linear relationship for L-dopa-HSA complex, and marks that the quenching is mainly static in the complex of L-dopa+ HSA.[38, 39] The Kq was calculated according to the Stern-Volmer equation:

$$F_0/F = 1 + k_q t_0 [Q] = 1 + K_D [Q] \quad -[2]$$

where F and F_o are the fluorescence intensities in the presence and absence of quencher, [Q] is the quencher concentration, and K_D is the Stern-Volmer quenching constant (Kq), which can be written as $K_D = kqt0$; where kq is the bimolecular quenching rate constant and t_0 is the lifetime of the fluorophore in the absence of quencher, lifetime of fluorophore for HSA is 5.6 ns. [40] The quenching constant (Kq) for L-dopa is calculated (Fig.2) to be 2.6×10^{13} M^{-1} s^{-1}. As these value is much greater than the maximum collisional quenching constant 2.0×10^{10} M^{-1} s^{-1}, thus the static quenching mechanism is ubiquitous in this complex of HSA-L-dopa.

To analysis the binding constants and number bound L-dopa molecules to HSA, a modified Stern- Volmer equation is used. [22, 23, 36, 41]

$$\log\left[\left(F_0 - F\right) \div F\right] = \log K_s + n \times \log[Q] \quad -[3]$$

Where Q, n and K_s are the quencher concentration, number of binding sites and binding constant, respectively. The results indicate a good linear relationship. The number of binding ligands was calculated to be 0.9 for L-dopa implying that HSA interact with L-dopa in a one- to-one ratio (Fig.1B). Further, the binding constants of L-dopa were calculated from the intercept as 2.3± 0.01×10^4 M^{-1} which indicates strong binding of L-dopa to HSA. Interestingly, there is a good correlation with the computationally calculated binding constant as 3.5×10^3 M^{-1}. Thus, this result was in prudent agreement with the experimental data. All the natural compounds bind in similar manner to HSA were published recently from our group on betulinic acid, feruloyl

masalinic acid, trimethoxy flavone, coumaroyltyramine and asiatic acid and their binding constants were K_{BA} = 1.685 ±0.01 × 10^6 M^{-1}, K_{FMA} =1.42±0.01 × 10^8 M^{-1},K_{TMF} = 1.0±0.01 × 10^3 M^{-1}, and KCT = 4.5±0.01 × $10^5 M^{-1}$, K_{AsA}= 3.86 ± 0.01×10^4 M^{-1} respectively.[11, 21, 29, 36, 42] Furthermore, the standard free energy is calculated by following equation.

$$\Delta G^\circ = -RT \ln K \qquad \text{-[4]}$$

ΔG is free energy, K is the binding constant at the corresponding temperature, which can be obtained from fluorescence data, and R is the gas constant. Thus, the free energy change is -5.9 kcal M^{-1} at 25 °C. We have also calculated the free energy (-4.6 kcal M^{-1}) from computation modeling and results are in agreement with the experimental data. However, the lower free energy is perhaps hydrophilic interactions formed between L-dopa and HSA complex. Furthermore, the free energy calculated value of -5.9Kcal/mol is directly associated with dissociation constant, Kd =4.3×10^{-5}M). In addition, similar types of interactions such as hydrophilic and hydrogen bonding were observed with our recent studies of natural compounds, feruloyl maslinic acid, trimethoxy flavone, coumaroyltyramine and asiatic acid with HSA. [11, 21, 29, 36, 42]

However we have even checked the fluorescence emission of L-dopa with another important plasma protein, i:e α-1-acid glycoprotein (AGP) which is an acute phase protein and it is also called as orosomucoid. There is no binding of L-dopa with AGP (data not shown). Hence this indicates that the binding of L-dopa is specific to HSA as all drugs won't bind to AGP as it's a positive acute-phase protein, whereas HSA is negative acute-phase protein, a major carrier protein for wide variety of drugs in the blood circulation.

Effect of Site Markers on L-dopa Binding to HSA

The intrinsic fluorescence of HSA is due to presence of sole tryptophan residue (Trp214) in the hydrophobic cavity of subdomain IIA. In further, molecular displacement experiments were performed by using site specific markers of site I (phenylbutazone) and site II (ibuprofen), respectively. The fluorescence was measured for HSA along with site specific marker of ibuprofen or phenylbutazone with equal concentration (1 μM) of protein and site specific marker. To this complex (HSA+ ibuprofen) increasing concentration of L-dopa was titrated and resulted quenching of fluorescence emission was observed. The binding constant of L-dopa-HSA complex was found to be $2.3 \pm 0.01 \times 10^4$ M^{-1} whereas with phenylbutazone and ibuprofen site markers showed as $9 \pm .02 \times 10^2$ M^{-1} and $2.1 \pm .01 \times 10^4$ M^{-1} respectively. The binding constant in presence of ibuprofen is close to that of L-dopa-HSA complexes value which was $2.3 \pm 0.01 \times 10^4$ M^{-1}. The observed fluorescence emission decrease upon increase in the concentration of L-dopa with HSA-ibuprofen indicates that there is a competition between the L-dopa and HSA. Whereas the binding constant obtained for L-dopa titrated with HSA-phenylbutazone is negligible (data not shown). These results show that L-dopa displaced ibuprofen from which it has little effect on binding of ibuprofen to HSA (Fig.3). Thus, these results indicate that displacement experiment confirms that the L-dopa is bound to IIIA subdomain of HSA which is Sudlow's site II of HSA.[43, 44]

Conformational studies of HSA-L-dopa complexes

In order to know the secondary structure HSA and its conformational changes upon binding of L-dopa, the CD could be one of the best techniques. CD is proven to be the ideal technique to monitor the changes in the protein ligand complex.[15] At room temperature the CD spectroscopy

was measured to understand the secondary structure elements and structural stability of the HSA upon L-dopa binding to HSA. Two negative bands at 208 and 218nm are exhibited by CD spectra of HSA in the ultraviolet region.[27, 29, 36, 42, 45] Various concentrations of L-dopa were titrated with free HSA depicts decreased in far-UV-CD without any changes in the peaks shift. This indicates that L-dopa induce a decrease in the α-helix content of the protein. Further, a slight change in the secondary structural elements of HSA with the highest concentration of L-dopa (0.009mM) was observed at room temperature (Fig. 4). Secondary structural element were calculated by using the CDNN 2.2 software and the free HSA secondary structure consists of ~58% α-helix, ~20% β-sheets and ~22% random coils, which are in agreement with the earlier work. [29, 42, 45, 46] From the above mentioned method it was found that complexation of HSA with L-dopa (0.009 mM), the α-helical content of the protein decreased from 58±2.4 to 50.6±1.8 % with an increase in β -sheets from 20±0.73 to 24±0.1% and random coils 22±1.0 to 25.4±0.8 % respectively (Table 1). These results indicate that the partial unfolding of the secondary structure of protein upon complex formation. Also, the conformational change occurred due to microenvironment change around the Trp residue.

Molecular Docking Studies

HSA is a globular protein composed of 585 amino acids with three domains (I, II and III), and each domain is further subdivided into subdomains A and B. [2] The principal endogenous and exogenous ligands bind in the hydrophobic cavities in the subdomain IIA and IIIA, which refer to sites I and II of HSA. Here site I of HSA shows affinity for phenylbutazone, warfarin and various other ligands in the same way, site II shows affinity for ibuprofen, n-butyl p-aminobenzonate and flufenamic acid and other drugs. [3] The site specific marker experiment

reveals that L-dopa binds to site II (subdomain IIIA) of HSA. To define the binding site, in further molecular docking was employed by using Autodock software. The crystal structure of HSA was taken from the Protein Data Bank (PDB: 1AO6) as an authentic structure. A sum of 30 different conformations were generated through blind docking procedure, in which lowest free energy change ΔG^0 for L-dopa + HSA binding is -4.63 kcal.mol^{-1}, and the binding constant is $K_{L\text{-}dopa}$= 3.5 × 10 ^{3} M^{-1}. These results are nearly close to the experimentally measured values of ΔG^0 = -5.9 kcal M^{-1} and $K_{L\text{-}dopa}$ =2.3 ± .01× 10 ^{4} M^{-1}. Apparently, there is a slight difference in the binding constant and free energy values from experimental to computational, however, this values may expect because the solution structure conformation may be different from the computational values since computational values would be closer to the X-ray crystal structure. The L-dopa and HSA complex is stabilized by hydrogen bonds between the compound and the Glu492, Arg410 and Lys414 amino acid residue of protein with bond lengths of 2.01 Å, 2.66 Å , 1.82 Å and 2.00 Å, respectively. L-dopa interact specifically with different residues located on the subdomain IIIA of the HSA and whole complex is stabilized by hydrogen bonds (Fig.5). Therefore, the molecular docking and free energy calculation results suggested that L-dopa bound to HSA with both hydrophilic and hydrogen bond interactions. The docking results are in good agreement with the experimental results and revealed important interactions between Schiff base complex and HSA. The conformation with lowest docking energy is selected for following MD analysis.

Analysis of Molecular Dynamic Simulations

To evaluate the stability of lowest docked energy protein complex properties were examined by means of root mean square deviation (rmsd's), root mean square fluctuation (rmsf's) and radius

of gyration (R_g) of protein. In inclusion, the stability of the HSA-L-dopa complex justifies the valid docked conformer. The rmsd's, R_g and rmsf's values of atom in the unliganded and liganded protein with respect to initial structures were calculated along 10000ps trajectories (Fig.6A and Fig.6B;Fig.7A and 7B). The rmsd values of atoms in pure HSA and L-dopa-HSA complex was plotted from 0 to 10000 ps as shown in (Fig.6A). These results indicates that the rmsd of both systems of HSA and L-dopa-HSA complexes reaches equilibration and oscillates around in average value after 2000ps time and remained stable till end of the simulation indicating that the protein complex was stable thereafter. The rmsd values of atoms in HSA and L-dopa-HSA complexes were calculated from 3000-10000ps trajectory, where the data points were fluctuated for L-dopa-HSA complex, 0.4±0.056nm and pure HSA, 0.33±0.035nm. We resolve the radius of gyration (Rg) values of free HSA and HSA-L-dopa complex as shown in (Fig.6B). In both systems, Rg values were stabilized at about 3000 ps, indicating that the MD simulation achieved equilibrium after 3000 ps. Initially, the Rg values of both free HSA and HSA-L-dopa complex was 2.64 nm. The free HSA, HSA-L-dopa were stabilized at 2.57±0.03 nm, respectively (Fig.6B). The previous report showed the Rg value of HSA determined experimentally from neutron scattering in aqueous solution was 2.74 ± 0.035 nm, indicating that our MD simulations are identical to the experimental values. [47]Also, the present result is in close agreement with our previous report that β-sitosterol and betulinic acid stabilizes from 2.59 ± 0.03 to 2.40 ± 0.031nm and 2.59 ± 0.03 to 2.51 ± 0.01 nm for free HSA and the HSA complexes, respectively [28, 45]. In case earlier reports on synthesized compound like 7-hydroxy coumarin derivative the free HSA where it was 2.7nm , HSA−7HC-1, HSA−7HC-2, and HSA−7HC-3 complexes were stabilized at 2.52 ± 0.03, 2.45 ± 0.031, and 2.45 ± 0.031 nm, respectively .[15]Thus the above present results of L-dopa suggest that the radius of gyration value decreased

upon L-dopa complexation with respect to free HSA. The radius gyration of both HSA and HSA-L-dopa are approximately similar to each other which clearly indicate that there are mild conformational changes during the simulation. Our results clearly match the experimental evidence (CD data) that the protein conformational changes were observed while L-dopa is binding to the HSA. Local protein mobility was analyzed by calculating the time- averaged rmsf's values of free HSA and L-dopa- HSA complexes were plotted against residue numbers based on the 10000ps trajectory data shown in (Fig.7A and 7B). The profiles of atomic fluctuations were found to be very similar to those of HSA and HSA-L-dopa complexes. Our result clearly indicates that sub-domains IA, IB, IIA, IIB and IIIB of HSA have highest fluctuations, while sub-domains IIIA presented lower fluctuations. In addition to this, atomic fluctuations of the residues Arg410, Lys413, Lys414, Ser480, Glu492 , Asp494, Leu491, Ser489 and Val493 that are involved in binding and the surrounding residues of subdomain IIIA were analyzed to ratify the binding and rigidity of the site (Fig.8). Overall the fluctuations of subdomain IIIA and the fluctuations of residues at the binding site clearly suggests that the L-dopa specifically interacts with the drug-binding site 2 (subdomain IIIA) of HSA. Also, our experimental results proved by site specific marker showed that L-dopa specifically binds to site II (IIIA domain) of HSA (Fig.3). To determine the flexibility and stability of the lowest energy conformer we analyzed at various time periods with intervals of 2-10ns. Fig.8 depicts that at 2ns the mobility of L-dopa in the subdomain IIIA is slightly fluctuated up to 8ns and there are structural rearrangements of L-dopa along with the surrounding residues of IIIA sub domain of HSA and then it got stabilized at 10ns upon binding of L-dopa with HSA. Although there is not much variation on the rmsd's observed as whole there not much variation in the rigidity in the

binding site (Fig.6A). Here R_g data is very well supported by the structural rearrangement and variation of L-dopa-HSA complex (Fig.6B).

Conclusions

The phytochemical, L-3,4-dihydroxyphenylalanine binding with HSA was studied and identified a strong binding. This molecule quenches the fluorescence emission of HSA at 360 nm, due to L-dopa-HSA complexation. Using Stern-Volmer equation, the binding constant is determined to be $2.3\pm .01\times10^4$ M^{-1} and the standard free energy change was found to be -5.92 $kcalM^{-1}$. Further, the molecule causes conformational changes such that the α-helix content decreases with increase in its concentration. At lower concentrations of the drug, the complex shows less conformation change. But, at final concentration (0.009mM) of drug, partial destabilization of α-helical content of HSA and HSA-L-dopa complexes are 58±2.4 to 50.6±1.8%. The conformational changes may cause the unfolding of HSA molecule upon binding of L-dopa, which is not significant enough to lose its stability and is further supported by molecular dynamics studies**.** Molecular docking studies show that the binding of L-dopa is at the sub-domain IIIA, mostly by forming hydrogen bonds with hydrophilic amino acids. The free energy and binding constant values coincides for both experimental and *in silico* analysis. It clearly suggests that HSA-L-dopa complex is more stable which is clearly evident from the hydrophilic interactions. Molecular displacement studies with phenylbutazone and ibuprofen shows that L-dopa binds to drug site II of subdomain IIIA which is in agreement with docking studies.

Furthermore, simulation data shows that the HSA-L-dopa complex reaches equilibration state at around 2 ns and RMSF which is not significantly altered from HSA. In the evidence provided here shows that HSA acts as a good carrier molecule for L-dopa which helps in development of L-dopa in designing pharmaceutical important drugs.

ACKNOWLEDGMENTS

This work was supported by Department of Science and Technology (No. SR/SO/BB-0123/2010 and DST-FIST), DBT-CREBB, India and UPE-2, University of Hyderabad. We thank CIL and BIF, University of Hyderabad, for CD and Bioinformatics facilities.

References

1. T. Peters Jr, *All about albumin: biochemistry, genetics, and medical applications*, Academic Press, 1995.
2. D. Carter, X.-M. HE, S. H. Munson, P. D. Twigg, K. M. Gernert, M. B. Broom and T. Y. Miller, *Science*, 1989, 244, 1195-1198.
3. G. Sudlow, D. Birkett and D. Wade, *Mol. Pharmacol.*, 1976, 12, 1052-1061.
4. S. Curry, H. Mandelkow, P. Brick and N. Franks, *Nat. Struct. Mol. Biol.*, 1998, 5, 827-835.
5. S. Curry, P. Brick and N. P. Franks, *Biochimica et Biophysica Acta (BBA)-Molecular and Cell Biology of Lipids*, 1999, 1441, 131-140.
6. X. M. He and D. C. Carter, *Nature*, 1992, 358, 209-215.

7. A. Varshney, P. Sen, E. Ahmad, M. Rehan, N. Subbarao and R. H. Khan, *Chirality*, 2010, 22, 77-87.

8. S. Sugio, A. Kashima, S. Mochizuki, M. Noda and K. Kobayashi, *Protein Eng.*, 1999, 12, 439-446.

9. J. Ghuman, P. A. Zunszain, I. Petitpas, A. A. Bhattacharya, M. Otagiri and S. Curry, *J. Mol. Biol.*, 2005, 353, 38-52.

10. F. Zsila, *Mol. Pharm.*, 2013, 10, 1668-1682.

11. R. Subramanyam, M. Goud, B. Sudhamalla, E. Reddeem, A. Gollapudi, S. Nellaepalli, V. Yadavalli, M. Chinnaboina and D. G. Amooru, *Journal of Photochemistry and Photobiology B: Biology*, 2009, 95, 81-88.

12. A. Garg, D. M. Manidhar, M. Gokara, C. Malleda, C. S. Reddy and R. Subramanyam, *PLoS ONE*, 2013, 8, e63805.

13. U. Kragh-Hansen, V. T. G. Chuang and M. Otagiri, *Biol. Pharm. Bull.*, 2002, 25, 695-704.

14. K. L. Hein, U. Kragh-Hansen, J. P. Morth, M. D. Jeppesen, D. Otzen, J. V. Møller and P. Nissen, *J. Struct. Biol.*, 2010, 171, 353-360.

15. D. P. Yeggoni, M. Gokara, D. Mark Manidhar, A. Rachamallu, S. Nakka, C. S. Reddy and R. Subramanyam, *Mol. Pharm.*, 2014, 11, 1117-1131.

16. B. Gautam, V. Vadivel, W. Stuetz and H. K. Biesalski, *Int. J. Food Sci. Nutr.*, 2012, 63, 242-245.

17. R. A. Hauser and T. A. Zesiewicz, *Med. Clin. North Am.*, 1999, 83, 393-414.

18. I. Gulcin, *Amino Acids*, 2007, 32, 431-438.

19. S. Prasad, A. Kulshreshtha and T. N. Qureshi, *Pakistan Journal of Nutrition*, 2009, 8, 551-557.

20. G. Boden, L. Lundy and O. Owen, *Neuroendocrinology*, 1972, 10, 309-315.

21. R. Subramanyam, A. Gollapudi, P. Bonigala, M. Chinnaboina and D. G. Amooru, *Journal of Photochemistry and Photobiology B: Biology*, 2009, 94, 8-12.

22. F. Zsila, Z. Bikádi and M. Simonyi, *Biochem. Pharmacol.*, 2003, 65, 447-456.

23. J. Min, X. Meng-Xia, Z. Dong, L. Yuan, L. Xiao-Yu and C. Xing, *Journal of Molecular Structure*, 2004, 692, 71-80.

24. G. M. Morris, D. S. Goodsell, R. S. Halliday, R. Huey, W. E. Hart, R. K. Belew and A. J. Olson, *Journal of computational chemistry*, 1998, 19, 1639-1662.

25. G. Jones, P. Willett and R. C. Glen, *J. Mol. Biol.*, 1995, 245, 43-53.

26. G. M. Morris, R. Huey, W. Lindstrom, M. F. Sanner, R. K. Belew, D. S. Goodsell and A. J. Olson, *Journal of computational chemistry*, 2009, 30, 2785-2791.

27. D. P. Yeggoni, M. Gokara, D. Mark Manidhar, A. Rachamallu, S. Nakka, C. S. Reddy and R. Subramanyam, *Mol. Pharm.*, 2014.

28. C. Malleda, N. Ahalawat, M. Gokara and R. Subramanyam, *Journal of molecular modeling*, 2012, 18, 2589-2597.

29. M. Gokara, T. Malavath, S. K. Kalangi, P. Reddana and R. Subramanyam, *J. Biomol. Struct. Dyn.*, 2014, 32, 1290-1302.

30. W. R. Scott, P. H. Hünenberger, I. G. Tironi, A. E. Mark, S. R. Billeter, J. Fennen, A. E. Torda, T. Huber, P. Krüger and W. F. van Gunsteren, *The Journal of Physical Chemistry A*, 1999, 103, 3596-3607.

31. L. D. Schuler, X. Daura and W. F. Van Gunsteren, *Journal of Computational Chemistry*, 2001, 22, 1205-1218.

32. J. Li, X. Liu, C. Ren, J. Li, F. Sheng and Z. Hu, *Journal of Photochemistry and Photobiology B: Biology*, 2009, 94, 158-163.

33. A. Sułkowska, *Journal of molecular structure*, 2002, 614, 227-232.

34. Y. V. Il'ichev, J. L. Perry and J. D. Simon, *The Journal of Physical Chemistry B*, 2002, 106, 452-459.

35. P. Kandagal, S. Kalanur, D. Manjunatha and J. Seetharamappa, *J. Pharm. Biomed. Anal.*, 2008, 47, 260-267.

36. M. Gokara, B. Sudhamalla, D. G. Amooru and R. Subramanyam, *PLoS ONE*, 2010, 5, e8834.

37. D. Agudelo, P. Bourassa, J. Bruneau, G. Berube, E. Asselin and H.-A. Tajmir-Riahi, *PLoS ONE*, 2012, 7, e43814.

38. Zhang, Q. Que, J. Pan and J. Guo, *Journal of Molecular Structure*, 2008, 881, 132-138.

39. S. R. Feroz, S. B. Mohamad, Z. S. Bakri, S. N. Malek and S. Tayyab, *PLoS ONE*, 2013, 8, e76067.

40. N. Tayeh, T. Rungassamy and J. R. Albani, *J. Pharm. Biomed. Anal.*, 2009, 50, 107-116.

41. L. Liang, H. Tajmir-Riahi and M. Subirade, *Biomacromolecules*, 2007, 9, 50-56.

42. S. Neelam, M. Gokara, B. Sudhamalla, D. G. Amooru and R. Subramanyam, *The Journal of Physical Chemistry B*, 2010, 114, 3005-3012.

43. S. S. Kalanur, J. Seetharamappa and V. K. A. Kalalbandi, *J. Pharm. Biomed. Anal.*, 2010, 53, 660-666.

44. X. Wu, J. Liu, H. Huang, W. Xue, X. Yao and J. Jin, *Int. J. Biol. Macromol.*, 2011, 49, 343-350.

45. B. Sudhamalla, M. Gokara, N. Ahalawat, D. G. Amooru and R. Subramanyam, *The Journal of Physical Chemistry B*, 2010, 114, 9054-9062.

46. J.-S. Mandeville, E. Froehlich and H. A. Tajmir-Riahi, *J. Pharm. Biomed. Anal.*, 2009, 49, 468-474.

47. M. Kiselev, G. IuA, G. Dobretsov and M. Komarova, *Biofizika*, 2001, 46, 423.

Figure legends:

Fig. 1 Fluorescence emission spectra of HSA-L-dopa in 0.1 M phosphate buffer with pH 7.2, λex = 285 nm, and temperature at 25°C. Free HSA (0.001 mM) and free HSA with different concentrations L-dopa from 0.001 to 0.009 mM. (B) Modified Stern Volmer, Plot of log (dF/F) against log [Q]. λex = 285 nm and λem = 360 nm. Insert, the chemical structure of L-dopa ($C_9H_{11}NO_4$,).

Fig. 2 To determine the static and dynamic quenching a modified Stern−Volmer plot was used for fluorescence quenching constants (Kq) HSA-L-dopa complex.

Fig. 3 Fluorescence emission of HSA-L-dopa in the presence of site specific marker ibuprofen. The concentration of HSA and ibuprofen is kept constant at 1μM while the concentration of L-dopa is varied from 1 to 9 μM.

Fig. 4 Circular dichroism spectra of HSA+L-dopa complex in PBS, at pH 7.2 and were recorded with a JASCO J-815 CD spectropolorimeter. A quartz cell with a path length of 0.02 cm was used.

Fig. 5 Schematic view of lowest binding energy docked conformation obtained from docking simulation (A) L-dopa bound to IIIA domain on HSA (protein and ligand colored blue, red, white and green, respectively) (B) By using pymol stereo view of L-dopa binding site to HSA IIIA domain in which L-dopa is rendered as capped sticks and surrounding residues as lines (ARG410, LYS413, VAL 493, ASP494, GLU492, LEU491, SER489 and LYS414) (C) The

hydrophobic and hydrophilic amino acid residues surrounding the probe L-dopa (D) Ligplot is used to the show the hydrophobic interactions of HSA with L-dopa.

Fig. 6 (A)The Root mean square deviation (nm) of unligand HSA and ligand HSA (HSA+L-dopa). (B) The time dependence of the radius of gyration (Rg) for the backbone atoms of unligand HSA and ligand HSA (HSA+L-dopa).

Fig. 7 (A) The RMSF values against residue numbers**.** The RMSF values of unligand HSA and HSA-L-dopa complex were plotted against residue numbers. (B) The profile of atomic fluctuations. Atomic fluctuations of unliganded HSA and HSA+L-dopa complex to the active site amino acid residues present in the IIIB subdomain of HSA which is Site II.

Fig. 8 Ligplot shows hydrophobic interaction with subdomain IIIA at different nanoseconds, for HSA+L-dopa.

Figure 1.

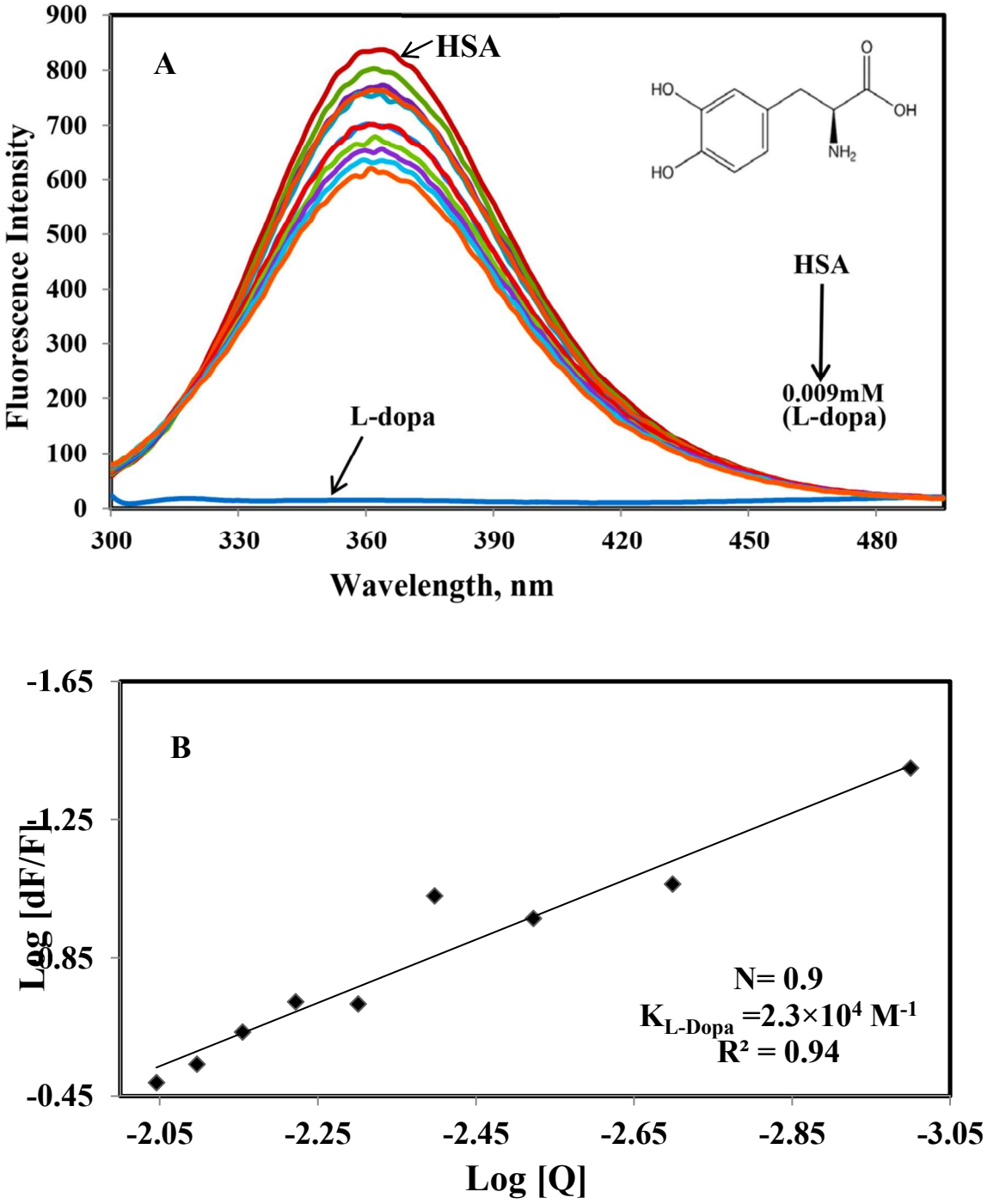

Figure 2.

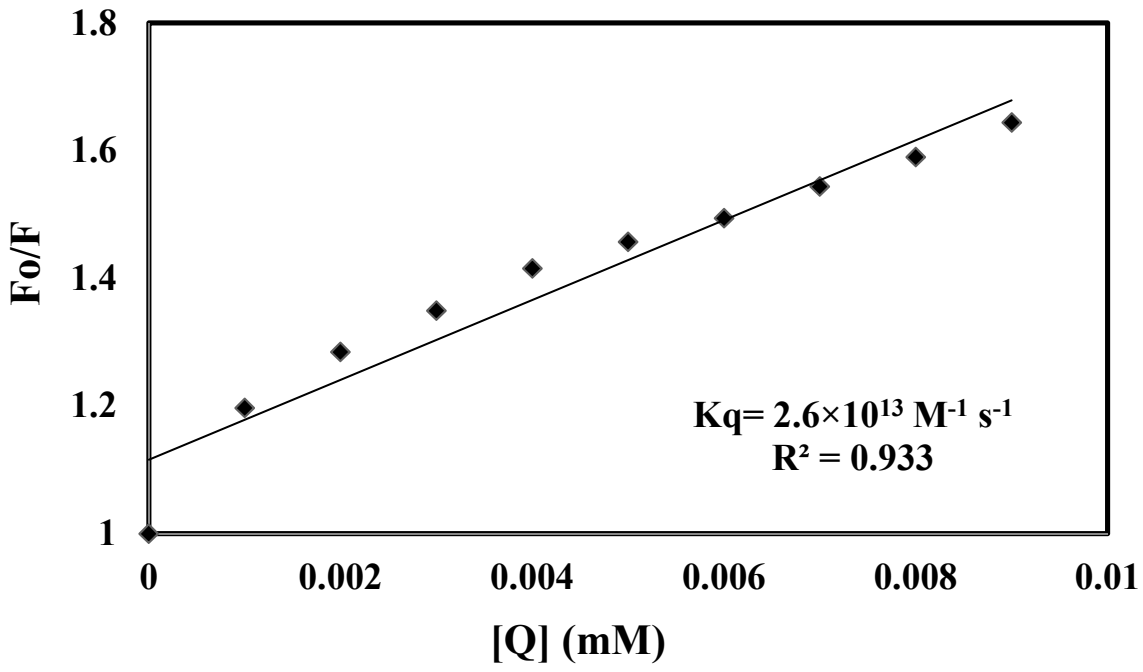

Figure 3.

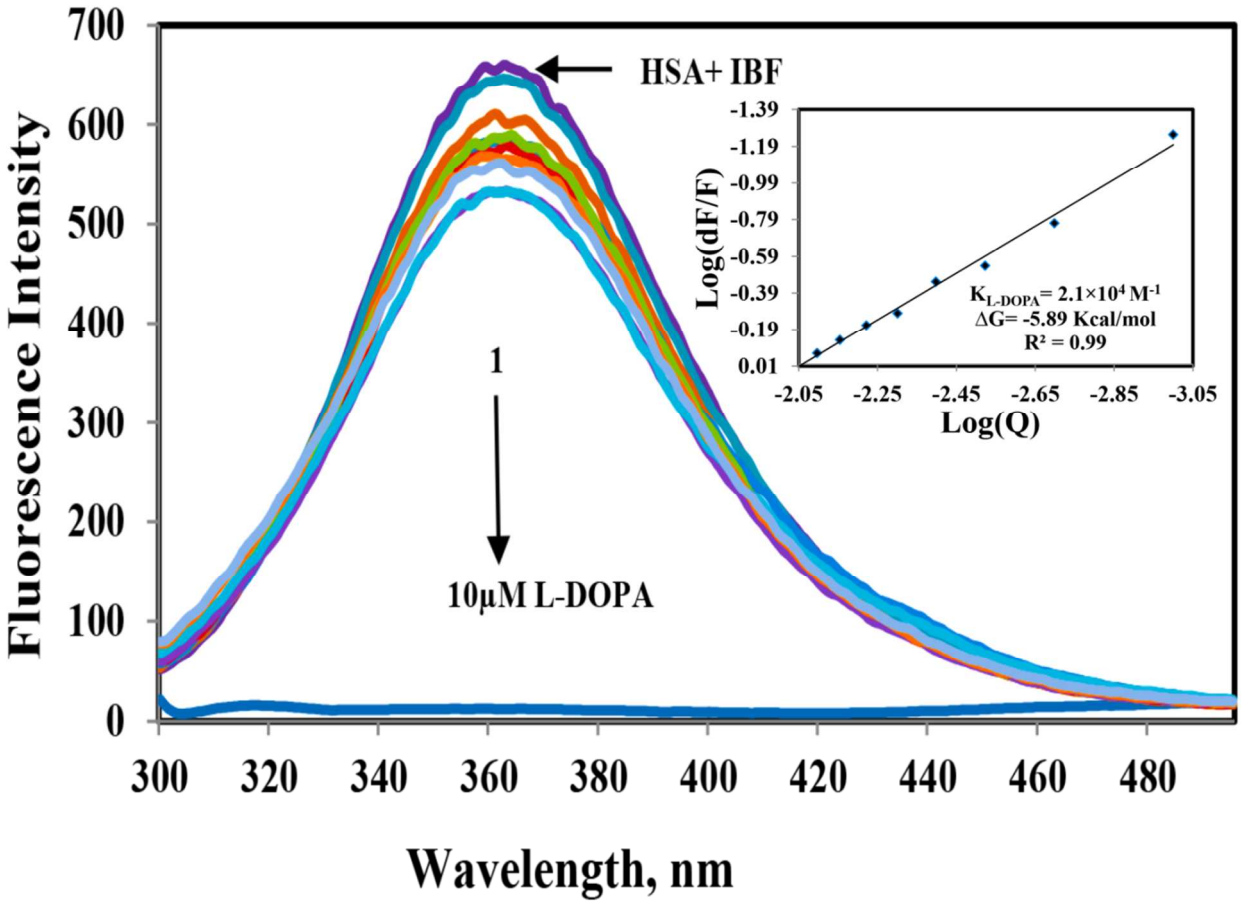

Figure 4.

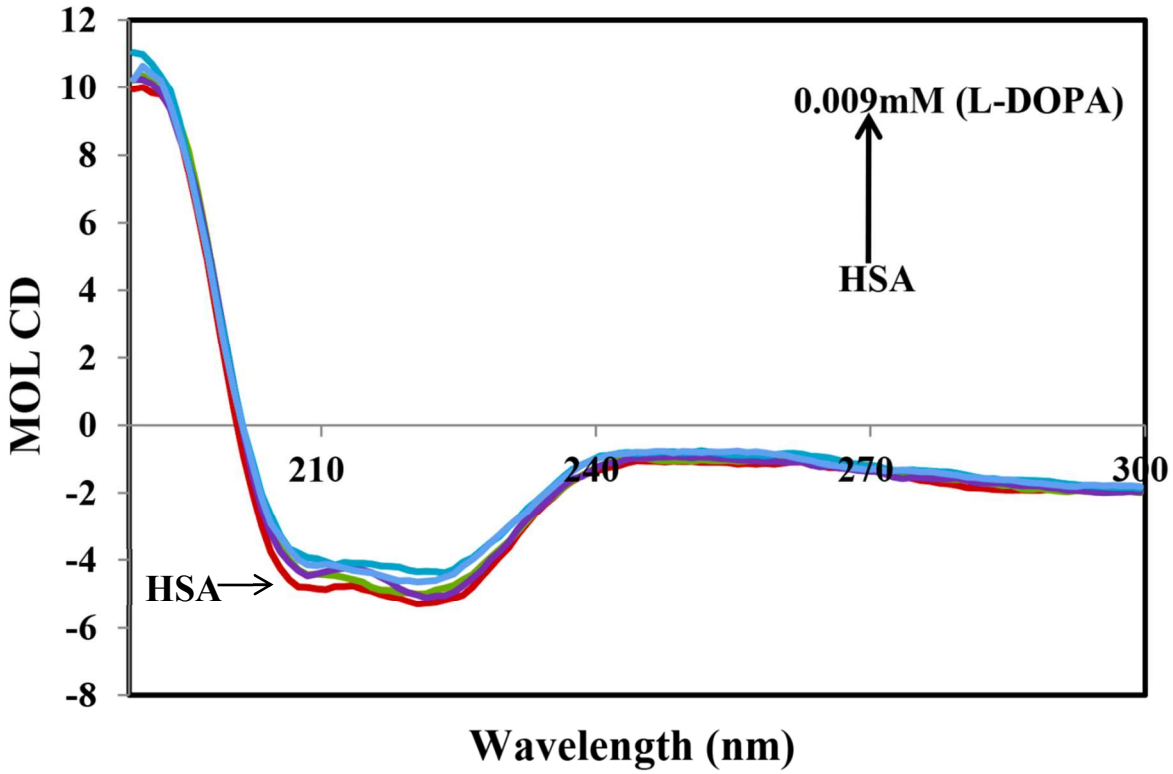

Figure 5.

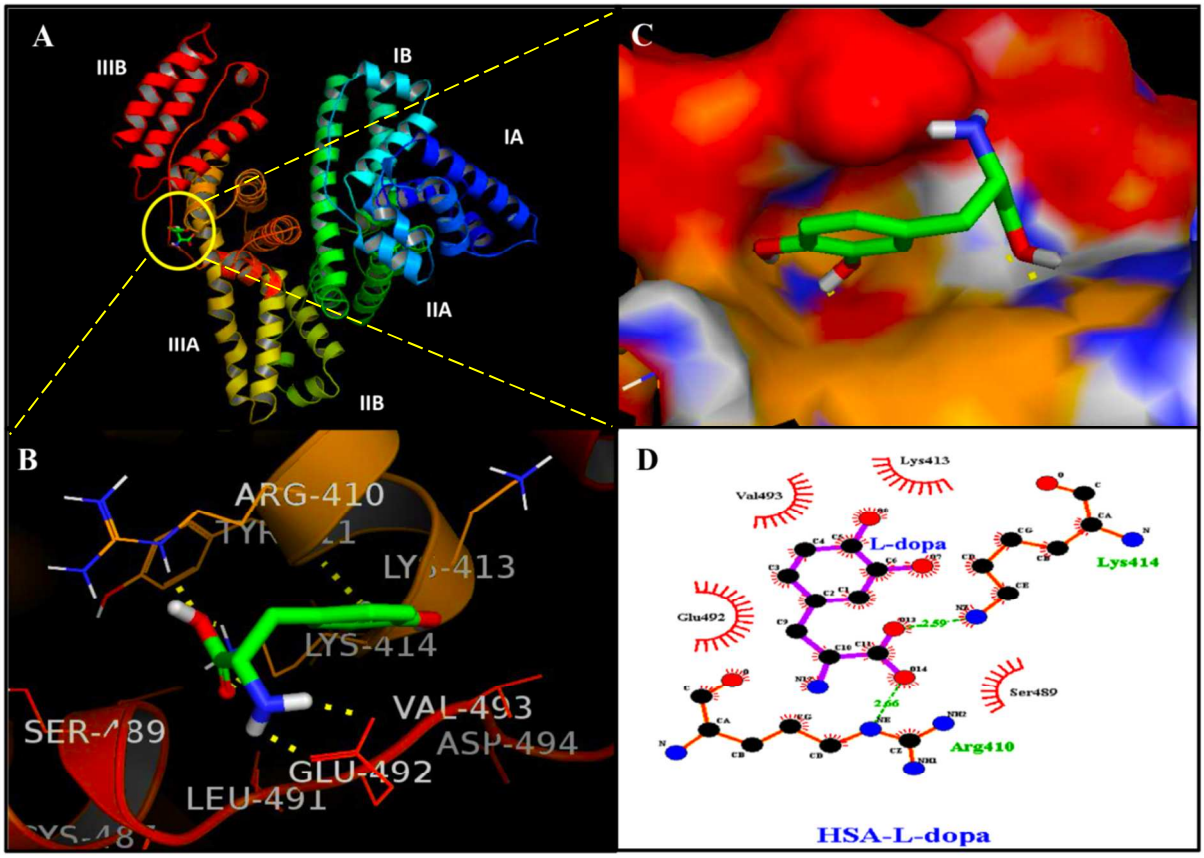

Figure 6.

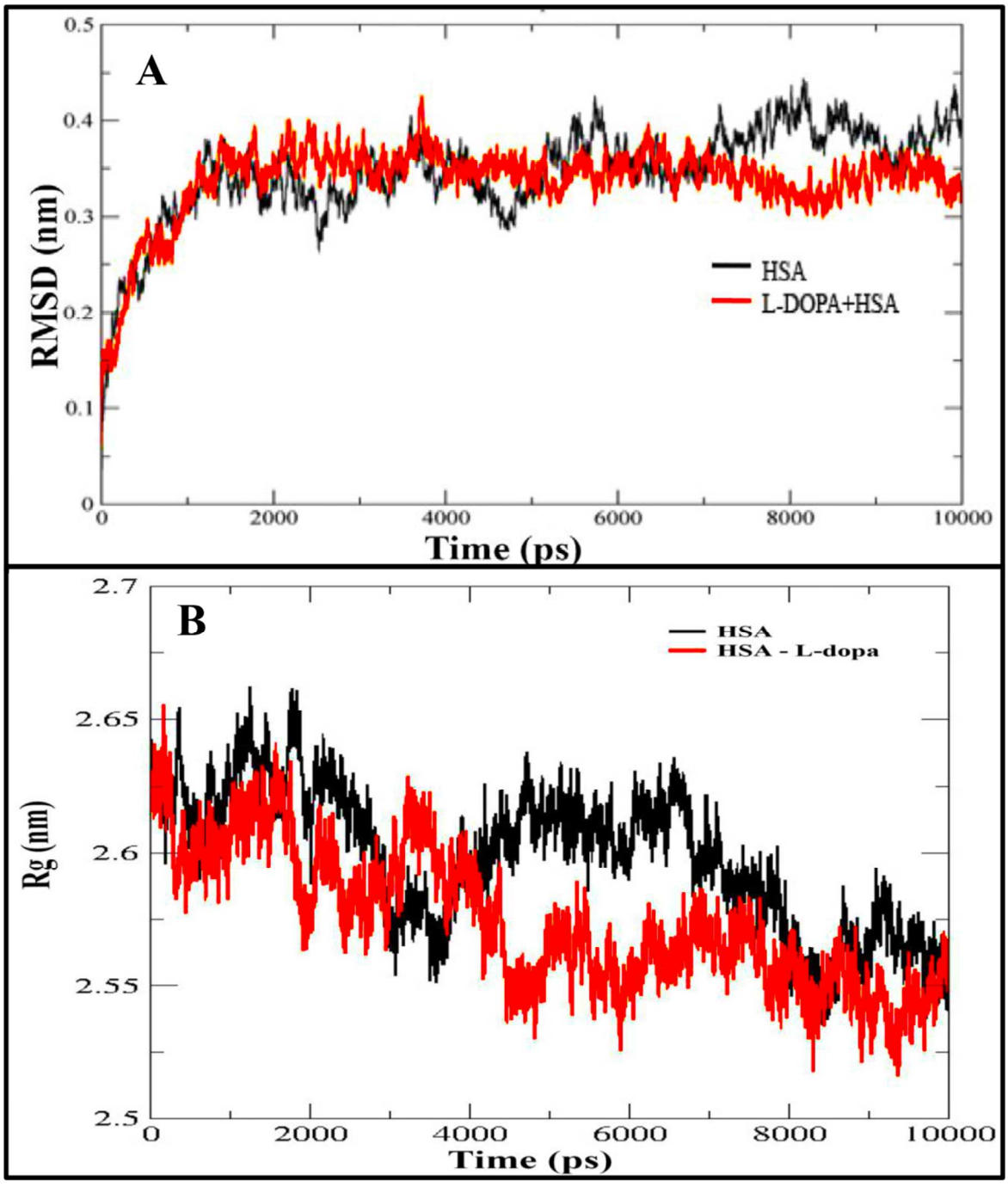

Figure 7.

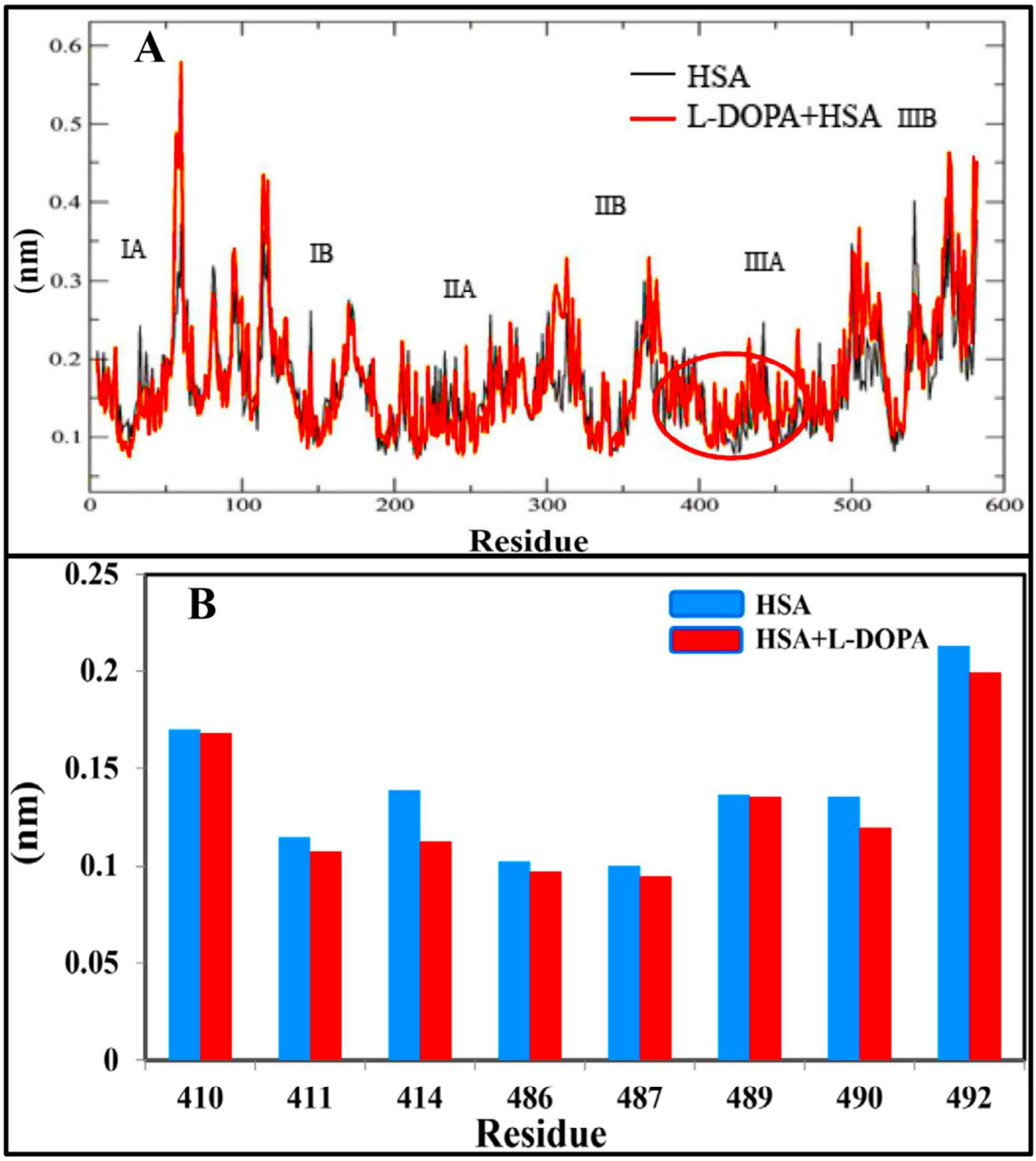

Figure 8.

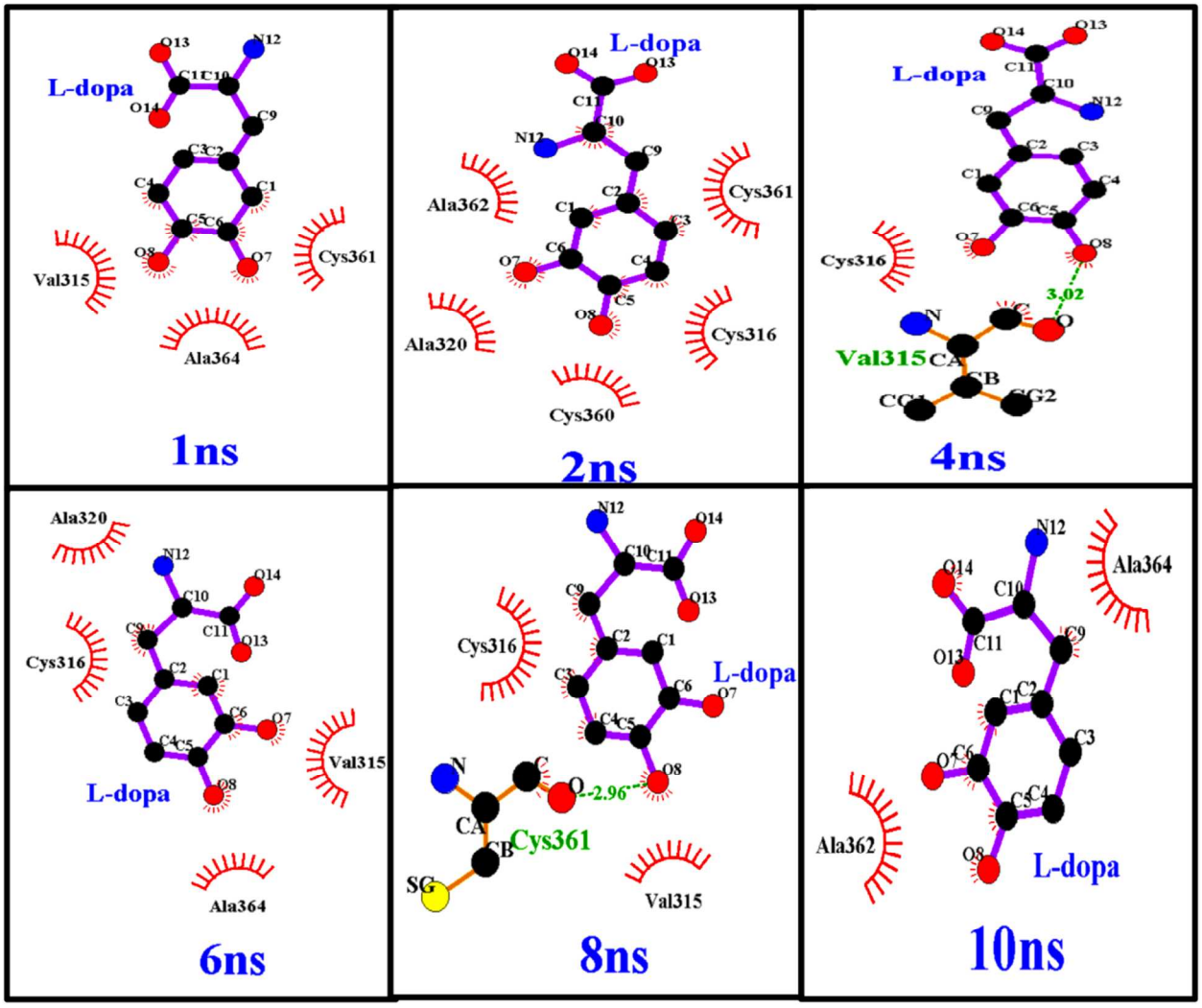

Table 1. Secondary structural analysis of HSA and HSA plus various concentrations (0.003, 0.005 and 0.009 mM) of L-dopa.

L-dopa	HSA(mM)	HSA+0.003(mM)	HSA+0.005(mM)	HSA+0.009(mM)
α-Helix%	58±2.4	55.4±2.03	53.4±2.04	50.6±1.8
β-Sheet%	20±0.73	21.8±0.6	22.3±0.8	24±0.1
Random coils%	22±1.0	22.8±0.6	24.3±0.4	25.4±0.8

On the basis of Figure 4, the data was analyzed by web-based software CDNN 2.2.